ELSEVIER

Journal of Power Sources 69 (1997) 55–60

JOURNAL OF POWER SOURCES

Effect of alloying elements on the copper-base anode for molten carbonate fuel cells

E.R. Hwang *, J.W. Park, Y.D. Kim, S.J. Kim, S.G. Kang

Department of Material Engineering, College of Engineering, Hanyang University, Seoul 133-791, South Korea

Received 14 October 1996; accepted 26 January 1997

Abstract

The effects of aluminium and chromium on the structural stability and the electrochemical performance of porous Cu–Ni anodes for the molten carbonate fuel cell (MCFC) are examined in a simulated MCFC anode environment (923 K, 80% H_2–20% CO_2). The addition of aluminium and chromium inhibits porous Cu–Ni anodes from being sintered because of the formation of aluminium oxide and chromium oxide on their surfaces. Electrochemical performance is evaluated in terms of anodic polarization in a half-cell system. At an anodic overpotential of 100 mV, the current density for H_2 oxidation of the Cu–Ni–Al anodes is about 85 mA cm^{-2}. The current densities of the Cu–Ni and Cu–Ni–Cr anodes were, however, 114 and 112 mA cm^{-2}, respectively. © 1997 Elsevier Science S.A.

Keywords: Molten carbonate fuel cells; Sintering; Electrochemical performance; Anodes

1. Introduction

The molten carbonate fuel cell (MCFC) operating at approximately 923 K has been extensively studied by many investigators because of its high efficiency and ability of utilization for a wide variety of fuels, such as coal gas and even natural gas. Nevertheless, it still needs substantial investigation before the commercialization stage is reached. One of the important problems to be solved is to secure the structural stability of the anode without losing its electrochemical performance. Porous nickel has been used as an anode for MCFC [1], but its sintering and creep resistance has not been satisfactory. It has been found [2] that the sintering resistance of nickel anodes can be increased remarkably by adding about 10 wt.% Cr. According to Kinoshita et al. [3], chromium reacts with the electrolyte (62mol%Li_2CO_3–38mol%-K_2CO_3) to form $LiCrO_2$ oxides that are collected at grain boundaries and form barriers against metal diffusion. The addition of aluminium oxide [4,5] also has been known to be effective in increasing the sintering resistance of nickel anodes since the internal dispersion of the oxide particles within the nickel phase impedes the sintering and creep deformation of nickel. Although nickel-based porous metal shows good performance as an anode material, nickel is relatively expensive. Accordingly, cheaper anode material, which can replace nickel, has been explored and copper has been found to be more suitable material than nickel. Copper is less expensive and more stable under accidental current overload than nickel because of its more positive potential. Furthermore, copper has higher electrical conductivity and greater resistance to carburization than nickel. On the other hand, the electrochemical performance of copper in molten carbonate salt, as well as the sintering resistance, are less favourable than those of nickel. Yuasa et al. [6] reported that the addition of nickel on the copper anode increased the electrochemical performance. In addition, an earlier study [7] performed by the present authors, showed that the electrochemical performance of a Cu–35wt.%Ni anode is almost the same as that of a nickel anode. Nevertheless, the structural stability of a Cu–35wt.%Ni anode is still less than that of a nickel anode. Therefore, in the present study, the effects of aluminium and chromium are investigated for increasing the structural stability without losing electrochemical performance of the porous Cu–35wt.%Ni anode.

2. Experimental

2.1. Preparation of anode specimens

Green sheets of Cu–35wt.%Ni and Cu–35wt.%Ni–*X* anodes containing aluminium or chromium up to 10 wt.%

* Corresponding author. Fax: +82 (2) 296 4560.

PII S0378-7753(97)02566-4

were prepared from a slurry of copper in future, nickel in future, aluminium, and chromium metal powders and an aqueous solution of carboxymethyl cellulose. Dendrite-type copper powder of particle size of 2–3 μm and filament-type nickel powder of the particle size of 2.2–2.8 μm, (both powders have high specific surface area) were used as the base materials. As alloying elements, flake-type aluminium powder of particle size of 10–20 μm and sphere-type chromium powder of particle size of 1–5 μm were mixed with the Cu–Ni slurry by ball milling for 24 h. The slurry was tape cast into a green sheet by using the doctor blade. The green sheet was then fabricated into a porous electrode plaque by sintering under a reduction environment of a H_2–N_2 mixture at 1073 K. Porous Cu–35wt.%Ni plaque and Cu–35wt %Ni–*X* plaques were used for the sintering and the determination of electrochemical performance of test specimens.

2.2. *Sintering test*

In order to investigate the structural stabilities of the present specimens, sintering tests were performed for up to 700 h under a simulated conditions of MCFC anode condition (923 K, 80%H_2–20%CO_2). The structural stabilities were examined in terms of porosity by measuring the change in density as a function of sintering time. The density changes were measured by the Archimedes method [8]. After performance of the sintering tests, the effects of aluminium and chromium on the sintering resistance (and thus the structural stability) of the Cu–35wt.%Ni electrode were examined by scanning electron microscopy (SEM), energy dispersive spectroscopy EDS) and X-ray diffraction (XRD) analyses. Porosity and pore-size distribution were determined using a mercury intrusion porosimeter.

2.3. *Electrochemical performance*

The electrochemical performance of the present specimens was determined in a half-cell as shown in Fig. 1. In the half-cell, each specimen was used as a working electrode and a mixture of 62 mol% lithium carbonate (Li_2CO_3) and 38 mol% potassium carbonate (K_2CO_3) was used as an electrolyte. The working gas was 80%H_2–20%CO_2; this simulated the MCFC anode atmosphere [9]. The overpotential of the working electrode was controlled with respect to the reference electrode. The latter was made of gold foil spot-welded to gold wire (diameter 0.5 mm) which was inserted in the mullite tube (inner diameter 5 mm). A mixed gas composed of 67% CO_2 and 33% O_2 was fed continuously into the reference electrode. A 0.5 mm diameter gold wire was used as the counter electrode. The electrolyte in the reference-electrode compartment was the same as that in the cell. In order to evaluate the electrochemical performance of the present specimens, the working electrode was polarized at a constant scan rate of 1 mV s^{-1} in the positive potential direction to 130 mV with respect to open-circuit potential. At the overpotential of 100 mV, the anodic current for H_2 oxidation was

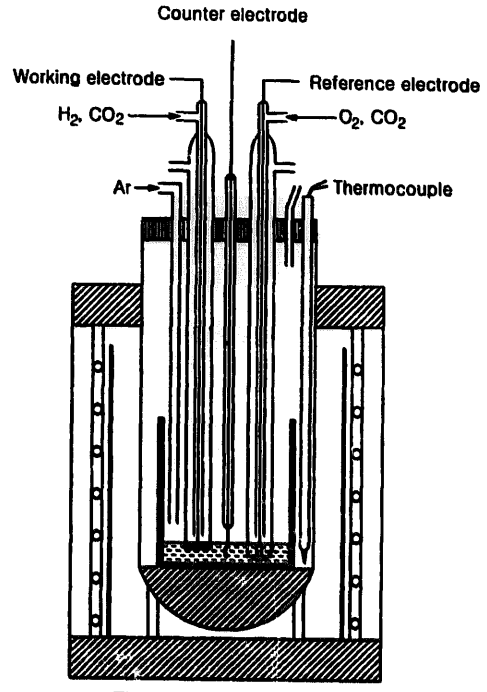

Fig. 1. Schematic of half-cell.

examined for electrochemical performance. Anode polarizations were measured by using a EG&G Model 273 potentiostat/galvanostat.

3. Results and discussion

3.1. *Structural stability*

Fig. 2 shows the initial pore-size distributions, median pore diameters, and porosities of Cu–35wt.%Ni and Cu–35wt.%Ni–*X* (*X* = Al or Cr) specimens before sintering test. The cumulative volume percent of pores in the 3–20 μm size range, which is the desired pore-size distribution for an MCFC anode, was about 90% for both Cu–Ni and Cu–Ni–Cr specimens, but 75–85% for the Cu–Ni–Al specimen. Therefore, it was considered that the pore-size distribution of the present specimens were satisfactory. The addition of 10 wt.% aluminium to the Cu–35wt.%Ni specimen increased the median pore diameter from 8.9 to 12.9 μm and the porosity from 65.5 to 68.1%, whereas the addition of 10 wt.% chromium decreased the median pore diameter from 8.9 to 5.5 μm and the porosity from 65.5 to 64.7%. The changes in median pore diameter and porosity by addition of aluminium and chromium are considered to be due to the difference in particle size. In other words, the initial pore size of the Cu–35wt.%Ni specimen increased when the aluminium powder of larger particle size was introduced, and decreased when the chromium powder of smaller particle size was introduced into the specimen. The typical MCFC anode has a median pore diameter of approximately 4–8 μm with the porosity of 55–70% [10]. Even though the median pore diameter of the Cu–Ni–Al specimen was slightly larger than that of the typ-

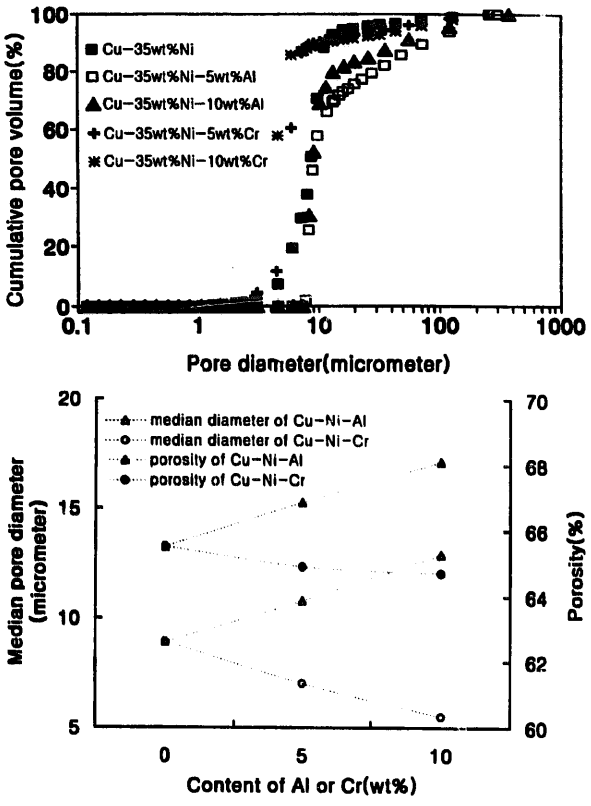

Fig. 2. Effects of aluminium and chromium contents on initial pore-size distributions and porosity of a Cu–35wt.%Ni specimen.

ical MCFC anode, the porosities of the Cu–Ni–Al and Cu–Ni–Cr specimens were adequate for an MCFC anode.

In Fig. 3, the percent increments of relative density of the present specimens with increasing aluminium and chromium contents are presented as a function of sintering time at 923 K in a H_2–CO_2 atmosphere. As can be seen in Fig. 3, the addition of aluminium or chromium up to 10 wt.% is effective in retarding the sintering of Cu–35wt.%Ni specimens; the relative density increased by 12.6±0.4% after sintering at 923 K for 700 h. The incremented increase in the relative density became smaller, however, with increasing aluminium and chromium content under the same conditions; the increment was 9.7±0.3% and 9.4±0.3% for Cu–35wt.%Ni–10wt.%Al and Cu–35 wt.%Ni–10wt.%Cr, respectively.

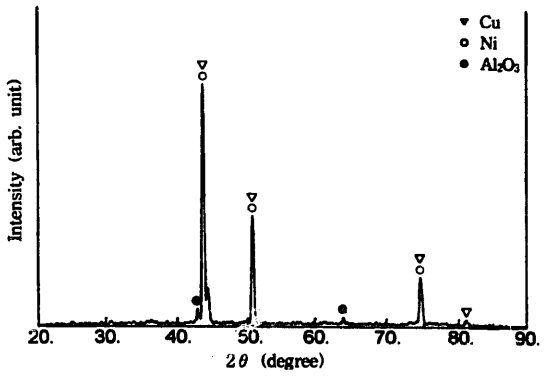

Fig. 4. XRD pattern of Cu–35wt.%Ni–10wt.%Al specimen after sintering for 700 h at 923 K.

When considering the experimental error, the difference between the relative densities of Cu–35wt.%Ni–10wt.%Al and Cu–35wt.%Ni–10wt.%Cr can be ignored. Thus, it is concluded that aluminium and chromium have almost the same effect on increasing the sintering of Cu–35wt.%Ni. Niikura et al. [11] reported that the large change in the microstructure of the MCFC anode due to sintering can be restrained by using a sintering-resistant material, e.g., as Ni–Al for which high structural stability is caused by the formation of aluminium oxide. For the oxidation reaction of aluminium, the equilibrium O_2 pressure at 923 K is approximately of the order to 10^{-50} bar [12]. Thus, aluminium is easily oxidized in an anode gas atmosphere where the O_2 partial pressure is about 10^{-23} bar. According to Iacovangelo [13], addition of chromium into a nickel anode increases the sintering resistance due to the formation of chromium oxide on the surface of the nickel phase. In the anode gas atmosphere, chromium in Ni–Cr alloy is selectively oxidized to Cr_2O_3 since the equilibrium O_2 partial pressure for oxidation of chromium is about 10^{-33} bar. The chromium oxide on the surface retards the surface diffusion of nickel and the loss of porosity. It is to be expected from the above thermodynamic consideration that only aluminium or chromium in Cu–Ni–X (X = Al or Cr) is oxidized during sintering in the anode environment (923 K, 80%H_2–20%CO_2). This was confirmed by XRD; the data for Cu–35wt.%Ni–10wt.%Al and Cu–35wt.%Ni–10wt.%Cr specimens after sintering for 700 h are shown in Figs. 4 and 5,

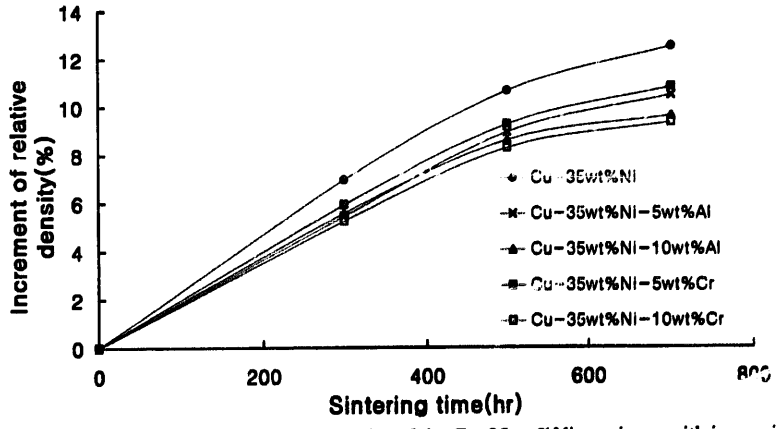

Fig. 3. Effects of Al and Cr content on the increment of relative density of the Cu–35wt.%Ni specimen with increasing sintering time at 923 K.

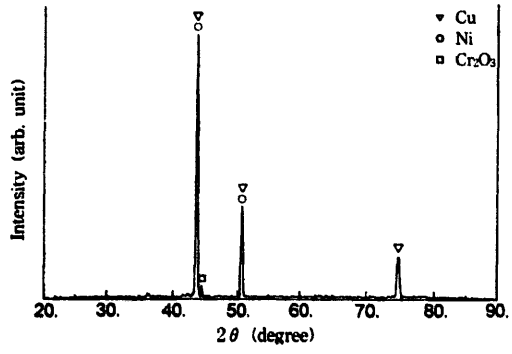

Fig. 5. XRD pattern of Cu–35wt.%Ni–10wt.%Cr specimen after sintering for 700 h at 923 K.

respectively. The oxides identified from analyses of the XRD patterns were Al_2O_3 in the case of the Cu–35wt.%Ni–10wt.%Al specimen and Cr_2O_3 in the case of the Cu–35wt.%Ni–10wt.%Cr specimen. In order to observe the microstructural changes, the sintered specimens were examined by using SEM. The microstructural changes of Cu–35wt.%Ni, Cu–35wt.%Ni–10wt.%Al and Cu–35wt.%Ni–10wt.%Cr specimens after sintering for 700 h. are shown in Fig. 6. The sintered Cu–35wt.%Ni specimens exhibit a well-necked structure. This type of structure is not displayed by the Cu–35wt.%Ni–10wt.%Al and Cu–35wt.%Ni–10wt.%Cr specimens. Therefore, it is confirmed that the aluminium and chromium oxides formed on the surface of Cu–Ni particle effectively inhibit the sintering of the Cu–35wt.%Ni specimen. Furthermore, it is also found from the above relative density measurement that the sintering resistance of Cu–35wt.%Ni increases with increasing contents of aluminium and chromium.

3.2. Electrochemical performance

The anodic polarization curves of the Cu–Ni–*X* anodes are shown in Fig. 7. The results show that the current density of

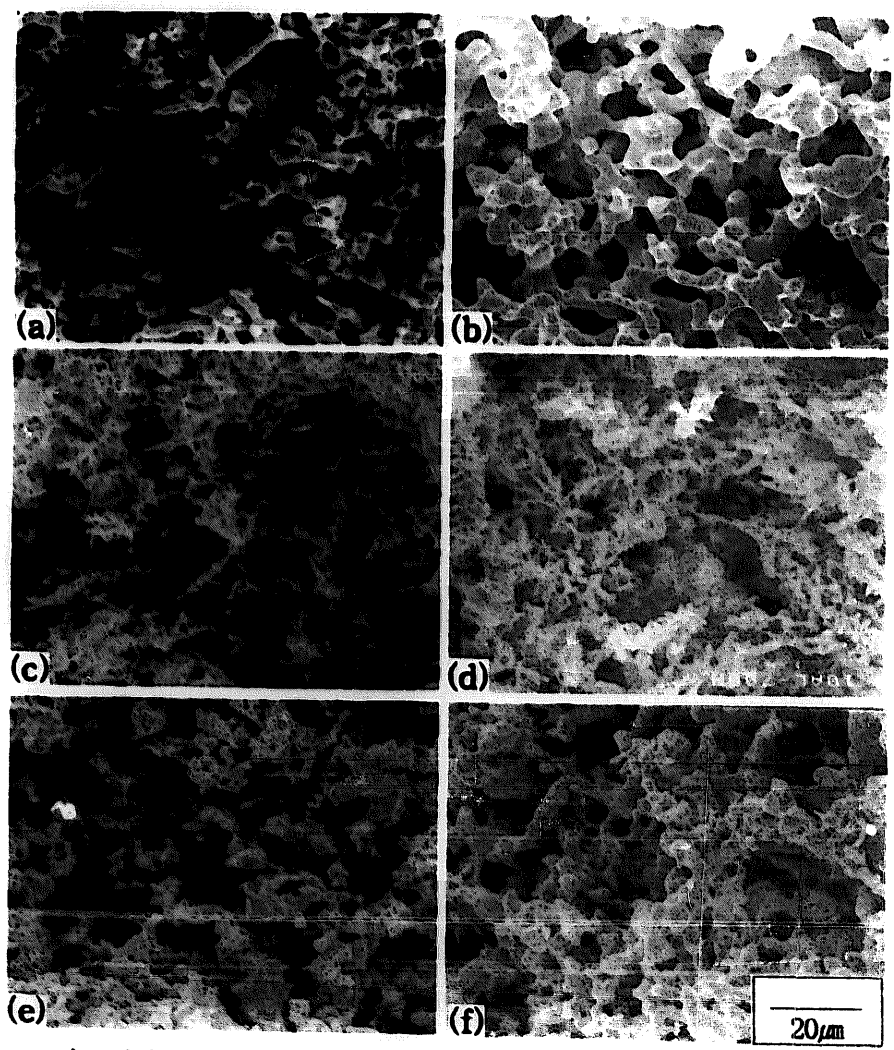

Fig. 6. SEM images of porous specimens before and after sintering for 700 h at 923 K: (a) Cu–35wt.%Ni before sintering; (b) Cu–35wt.%Ni after sintering; (c) Cu–35wt.%Ni–10wt.%Al before sintering; (d) Cu–35wt.%Ni–10wt.%Al after sintering; (e) Cu–35wt.%Ni–10wt.%Cr before sintering, and (f) Cu–35wt.%Ni–10wt.%Cr after sintering.

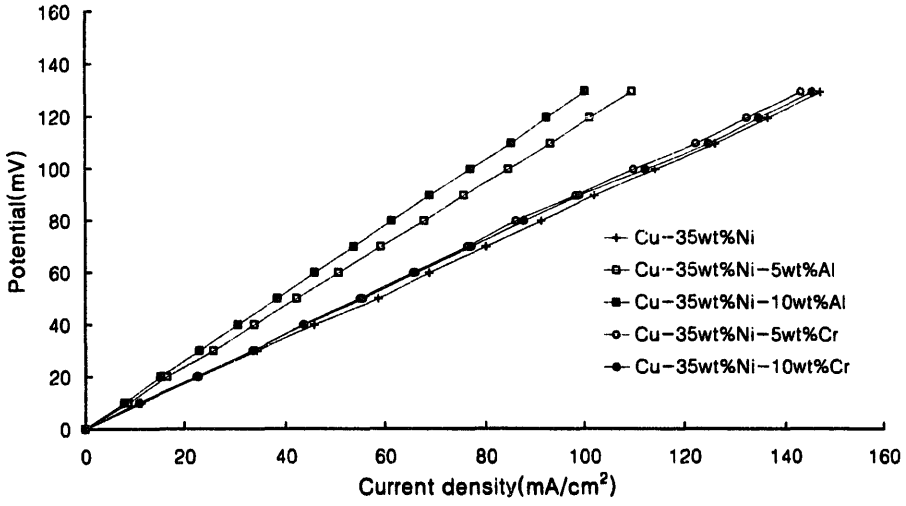

Fig. 7. Polarization behaviour of copper-base anodes under simulated MCFC anode conditions.

the Cu–35wt.%Ni–*X* anode is independent of the aluminium and chromium concentration up to 10 wt.%. The current density of the Cu–Ni anode is higher than those of the Cu–Ni–Al anodes, whereas it is almost the same as those of the Cu–Ni–Cr anodes. The current densities of Cu–35wt.%Ni anodes for H_2 oxidation at an overpotential of 100 mV are about 114 mA cm^{-2}, whereas those of the Cu–35wt.%Ni–Al and Cu–35wt.%Ni–Cr anodes are about 85 and 112 mA cm^{-2}, respectively. In order to explain the effect of addition of aluminium or chromium on the current density of the Cu–35wt.%Ni anode it is assumed that the current density of a porous anode depends mainly on the total specific impedance. From the linearity of polarization curves, the electrochemical properties of a given anode can be characterized by the total specific impedance as follows

$$i = \eta / Z \quad (1)$$

where i is the current density, η the anodic overpotential, and Z is total specific impedance per unit area of anode. Susuki and Wyrwa [14] reported that the impedance of an anode is inversely proportional to its inner surface area (determined by the BET method). It was observed that the porosity of a sintered specimen decreased with decreasing specific surface area [15]. As shown in Fig. 2, the Cu–Ni–Al specimen has a lower porosity than the Cu–Ni and Cu–Ni–Cr specimens. Thus, it is concluded that the low electrochemical performance of the Cu–Ni–Al anode is due to the small specific surface area.

4. Conclusions

From the present investigation, the following conclusions can be drawn.

1. The sintering resistance of Cu–35wt.%Ni increases with increasing content of aluminium and chromium. By contrast, there is no difference between aluminium and chromium in the effectiveness of increasing the sintering resistance of Cu–35wt.%Ni. The relative density of Cu–35wt.%Ni increases by 12.6±0.4%, whereas that of Cu–35wt.%Ni–10wt.%Al and Cu–35wt.%Ni–10wt.%Cr increases by 9.7±0.3% and 9.4±0.3%, respectively, after sintering at 923 K for 700 h.

2. In a half-cell test, the current density of Cu–35wt.%Ni–*X* anode is independent of the aluminium and chromium concentration up to 10 wt.%. The current density of the Cu–35wt.%Ni anode for oxidation of H_2 at an overpotential of 100 mV is 114 mA cm^{-2} and that of the Cu–35wt.%Ni–Cr anode is 112 mA cm^{-2}. On the other hand, the current density of the Cu–35wt.%Ni–Al anode is 85 mA cm^{-2}, which is about 75% lower than that of the Cu–35wt.%Ni and Cu–35wt.%Ni–Cr anodes. It is concluded that the low electrochemical performance of the Cu–35wt.%Ni–Al anodes is due to its small inner specific surface area.

References

[1] C.Y. Yuh and J.R. Selman, *J. Electrochem. Soc., 138* (1991) 3642.
[2] L.G. Marianowski, R.A. Donado and H.C. Maru, *US Patent No. 4 247 604* (27 Jan. 1981).
[3] S.S. Penner, *Assessment of Research Needs for Advanced Fuel Cells*, Pergamon, Oxford, 1986, p. 153.
[4] C.D. Iacovangelo, *J. Electrochem. Soc., 133* (1986) 1359.
[5] *Ext. Abstr., Fuel Cell Seminar, 23–26 Oct. 1988, Long Beach, CA, USA*, National Fuel Cell Coordinating Group.
[6] K. Yuasa, J. Nikura, T. Nishina and I. Uchida, *Denki Kagaku, 58* (1990) 856.
[7] J.W. Park, Y.D. Kim, E.R. Hwang, S.J. Kim and S.G. Kang, *J. Korean Inst. Sur. Eng., 28* (1995) 243.
[8] G.J. Shugar, R.A. Shugar, L. Bauman and R.S. Bauman, *Chemical Technicians' Ready Reference Handbook*, McGraw-Hill, New York, 2nd edn., 1981.

[9] T. Ogawa, K. Murata and T. Shirogami, *Denki Kagaku, 53* (1985) 626.
[10] J.R. Selman, in L.J.M.J. Blomen and M.N. Mugerwa (eds.), *Fuel Cell Systems*, Plenum, New York, 1993, p. 345.
[11] J. Niikura, K. Hatoh and T. Iwaki, *The Chemical Society of Japan*, (1989) 20.
[12] D.R. Gaskell, *Introduction to Metallurgical Thermodynamics*, McGraw-Hill, New York, 2nd edn., 1981, p. 287.
[13] C.D. Iacovangelo, *J. Electrochem. Soc., 133* (1986) 2410.
[14] L. Suski and J. Wyrwa, *J. Appl. Electrochem., 20* (1990) 625.
[15] S. Ogino, K. Matsumoto, S. Maruyama and T. Nakanishi, *Denki Kagaku, 52* (1984) 783.